

Chapter 1

Introduction

1.1 Motivation and History

The numerical simulation of hysteresis effects in ferromagnetic material plays an important role in many technological applications, which have been studied in the last decades. The quality of hysteresis models, measured as the correspondence of the simulated and experimental results, has been substantially improved in the last years. Careful implementation and increasing computer resources nowadays enable the application of hysteresis models within electromagnetic field simulations. Up to now, hysteresis models and their introduction in electromagnetic field simulation are still subject of ongoing research. Two basic ingredients are required here: an accurate hysteresis model, combined with an efficient numerical method for electromagnetic field simulation.

Models for the hysteresis of ferromagnetic materials based on the mutual interaction of the magnetic particles, were first developed by J.A. Ewing in 1890, who assumed that the magnetic dipoles can be freely turned according to the interactions between the magnetic moments and the interaction between the neighboring magnetic dipoles as well. On the basis of the experiment by Ewing, the hysteresis of ferromagnetic materials was expected to have qualitative and quantitative characteristics. The theory of quantum mechanics introduced by N. Bohr opens the way for simulating magnetic materials and moments on the basis of quantum theory. The analysis of the microstructure of materials and the physical interpretation of crystal structures from the point of magnetic field led to the theory of spin dynamics and the discovery of the optical properties of magnetic materials. The investigation of the microstructure of magnetic materials motivates the realization of weak magnetic materials and magnetic alloys with special properties. The next period of research is characterized by the development of different models based either on a mathematical or on a physical approach. First realization of dynamical hysteresis models for magnetic materials was presented by Y. Saito between 1982 and 1990 and M.L. Hodgdon in 1988. The Langevin model of paramagnetic materials based on Boltzmann statistics and the Weiss theory resulted in the Jiles-Atherton hysteresis model [23] [24] [25] in 1983 for the representation of the energy loss during the domain wall motion. The studies of Ewing were extended by several researchers and accumulated in the Preisach model [29]. Based on the studies of Preisach and Everett, a mathematical model for hysteresis based on a statistical characterization of material properties was developed by M.A.

Krasnoselskii and A.V. Pokrovskii in 1983. From this time on, a powerful development in the Preisach model started and resulted e.g. the books and papers of E. Della Torre [5], I.D. Mayergoyz [16], A. Visintin [28], O. Benadda, A. Ivanyi [17] and G. Bertotti [4] which are now considered standard reference. The first hysteresis model which also represents the vectorial property of the particle magnetization was the Stoner-Wohlfarth model [22] developed in 1947. A new generation of vector models was introduced by E. Della Torre [18] in 1998 to simplify the mathematical model considering the physical characteristics of ferromagnetic material.

Currently, research on hysteretic material and on hysteresis model is widely spread. Hysteretic materials are applied in many electrotechnical devices. New materials, e.g. compound materials, powder materials, rare-earth permanent magnet materials are applied which require increasingly accurate and efficient hysteresis models. On the basis of microscopic investigations of magnetic materials, the simulation of the nonlinear hysteresis characteristics can be realized by numerical techniques. With the development of the numerical computation in the twentieth century, discretization techniques for field simulation are classified as Finite Element Method (FEM), Boundary Element Method (BEM), Finite Difference in Time Domain (FDTD), and Finite Integration Technique (FIT) etc.. Hysteresis models can be introduced in electromagnetic field simulation based on a discretization of the geometry by arising a hysteresis model for each volumetric entity representing a piece of hysteretic material.

The FIT, presented by Weiland [51], [52], [53] in 1977, was first developed for frequency domain problems starting about three decades ago and later completed to a generalized scheme for the entire application range of Maxwell's equations. The FIT transfers the continuous Maxwell's Equations into a set of matrix equations, each of which is the discrete analogue of one of the original integral equations. The algebraic equations representing Maxwell's equations in the computational grid are called Maxwell-Grid-Equations. Important topological properties such as the curl-freeness of gradient fields and the divergence-freeness of curl fields carry over from the continuous level to the discrete level. The method allows different formulations for the discrete problem not only in frequency domain but also in time domain, which provides more flexibility to the numerical simulation scheme. These attractive features of the FIT motivated the numerical simulation of hysteresis effects in ferromagnetic materials by introducing hysteresis models into the FIT.

1.2 Overview

After introducing the motivation and the development history of hysteresis models and numerical computation for electromagnetic fields, the ferromagnetic hysteresis is introduced in Chapter 2. Starting from Maxwell's equations, the physics of magnetism including the domain structure in magnetic materials and the description of hysteresis loops during the magnetization process is introduced firstly. Then the Preisach models, classified as classical Preisach model, generalized Preisach model and vector model are shortly recalled. Then the Jiles-Atherton model is briefly introduced as a Langevin type hysteresis model.

In order to project Maxwell's equations from continuous space onto a finite grid space and to implement hysteresis models in electromagnetic field simulation based on the discretization of the finite grid space, the FIT is introduced in Chapter 3. The introduction of the

Finite Integration Implicit Time Domain formulation (FI^2TD) for magnetoquasistatic field problems prepares for hysteretic simulation.

The modelling and implementation of the hysteresis is introduced in Chapter 4. Two different models of hysteretic ferromagnetic material behavior are given: the Preisach model and the Jiles-Atherton model. The magnetic polarization update scheme and the hysteretic nonlinear update scheme are introduced combining the two hysteretic ferromagnetic material modelling and the Finite Integration Implicit Time Domain formulation, respectively. The polynomial interpolation from the measured first-order transition curves is described in order to numerically implement the Preisach model and the inverse Preisach model. The computation of hysteretic losses is discussed and given by the integration of the hysteresis loops. The Jiles-Atherton model is implemented by its inverse form in the hysteretic nonlinear update scheme. Although scalar Preisach models have been increasingly accurate and efficient in describing material behavior, in many cases the magnetizing processes is vectorial in nature. The simplified vector model as one of the most computationally efficient models is implemented and compared with the corresponding scalar model. A hybrid method combining the solutions from the overrelaxed polarization method and the underrelaxed Newton method at each iterative cycle is implemented and discussed. The purpose of the hybrid Newton-polarization method is to increase the robustness of the nonlinear iteration, without losing the quadratic speed of convergence in the vicinity of the solution. A 3D transient hysteretic test problem is used for assessing the properties of all of the modelling and implementation methods.

The selected example of Benchmark problem TEAM 32 as an application of the numerical simulation of hysteresis effects in ferromagnetic material is demonstrated in Chapter 5. Two different supply cases are used for assessing the properties of the modelling and implementation of the hysteresis for magnetoquasistatic field problems.

The thesis is concluded with a summary in Chapter 6.

Chapter 2

Ferromagnetic Hysteresis

Ferromagnetic hysteresis is an important behavior of magnetic materials. Its phenomena can affect all applications of magnetic cores from electrical machines to transformers. The physics of magnetism responsible for hysteresis and the adequate mathematical tools to its description are the basis for the theoretical and the numerical study of hysteretic effects in ferromagnetic material. The physics of magnetism has been introduced with various approaches in different works by Bozorth [1], Chikazumi [2], Jiles [3], Bertotti [4] etc.. The Preisach model and the Jiles-Atherton model are the most popular mathematical models for the description of hysteretic phenomena. They have been developed and implemented in many numerical simulations for years.

In this chapter, on the bases of Maxwell's equations, the physics of magnetism, ranging from pure theory of the domain structure in magnetic substances to a plain description of hysteresis loops during the magnetization process, is introduced. As the applied hysteretic model in this thesis work, the Preisach model is recalled in a short summary. The classical Preisach model is described concerning its geometric interpretation, the determination of the distribution function and the numerical implementation. After the discussion of the main properties of the Preisach model, some modified Preisach models, generalized from classical one are shortly mentioned, which overcome the certain limitation of the classical Preisach model. The hysteretic losses are also discussed here. The vector Preisach model is shortly introduced, which will be further discussed in Chapter 4 as well. The Jiles-Atherton model is a Langevin type hysteresis model. It incorporates physical principles in the determination of five material parameters according to the experimental data. The Jiles-Atherton model will be further studied in Chapter 4.

2.1 Maxwell's Equations

Maxwell's equations are the fundamental equations to describe macroscopic electromagnetic phenomena in continuous space. They reflect the relation between the electric field values (field strength \vec{E} and flux density \vec{D}) and magnetic field values (field strength \vec{H} and flux density \vec{B}). They can be written in integral form for arbitrary faces A and volumina V and their respective boundaries ∂A and ∂V for non-moving geometries as:

$$\int_{\partial A} \vec{E}(\vec{r}, t) \cdot d\vec{s} = - \iint_A \frac{\partial}{\partial t} \vec{B}(\vec{r}, t) \cdot d\vec{A}, \quad (2.1)$$

$$\int_{\partial A} \vec{H}(\vec{r}, t) \cdot d\vec{s} = \iint_A \left(\frac{\partial}{\partial t} \vec{D}(\vec{r}, t) + \vec{J}(\vec{r}, t) \right) \cdot d\vec{A}, \quad (2.2)$$

$$\iint_{\partial V} \vec{B}(\vec{r}, t) \cdot d\vec{A} = 0, \quad (2.3)$$

$$\iint_{\partial V} \vec{D}(\vec{r}, t) \cdot d\vec{A} = \iiint_V q(\vec{r}, t) \cdot dV. \quad (2.4)$$

Here, equation (2.1) takes into account Faraday's law and equation (2.2) is called Ampère's law. The third equation (2.3) states that the total magnetic flux crossing any closed, regular surface has zero balance and the fourth equation is called Gauss's law. Maxwell's equations can be written in differential form as well, the differential form is derived by applying the theorems of Gauss and Stokes to the integral forms [49].

The current density $J(\vec{r}, t)$ in the equation (2.2) is composed of

$$\vec{J}(\vec{r}, t) = \vec{J}_k(\vec{r}, t) + \vec{J}_q(\vec{r}, t) + \vec{J}_i(\vec{r}, t), \quad (2.5)$$

where the conduction current density $\vec{J}_k(\vec{r}, t) = \kappa \vec{E}$ arises in materials with electric conductivity κ from the existing electric field strength; the imposed current density $\vec{J}_i(\vec{r}, t)$ expresses the excitation of the problem and is independent of all field forces; the current density $\vec{J}_q(\vec{r}, t)$ is the current contribution of free charges with the charge density q moving at the speed \vec{v} .

The physical characteristics of materials are described by constitutive relations, which relate the electric and magnetic flux densities (\vec{D} and \vec{B}) to the electric and magnetic field strengths (\vec{E} and \vec{H}). In the general case, the constitutive equations are

$$\vec{D} = \varepsilon_0 \vec{E} + \vec{P}, \quad (2.6)$$

$$\vec{B} = \mu_0 (\vec{H} + \vec{M}), \quad (2.7)$$

where the electric polarization \vec{P} and the magnetization \vec{M} of the material can be used in dispersive, anisotropic, nonlinear and hysteretic cases. For linear materials, the electric polarization is $\vec{P} = \varepsilon_0 \chi_e \vec{E}$, where χ_e is the electric susceptibility, and the magnetization is $\vec{M} = \chi_m \vec{H}$, with the magnetic susceptibility χ_m . In the more general case, we have

$$\vec{P} = \varepsilon_0 \chi_e \vec{E} + \vec{P}_r, \quad (2.8)$$

$$\vec{M} = \chi_m \vec{H} + \vec{M}_r. \quad (2.9)$$

The description of the material characteristics in the electromagnetic field calculation is extended by the independent permanent polarization \vec{P}_r and independent permanent magnetization \vec{M}_r . The physical characterization of magnetic materials is the general subject of this thesis and will be discussed in the following sections.

2.2 Physics of Magnetism

2.2.1 Magnetic Materials

There are various types of magnetism. Each of them is characterized by its own magnetic properties. The various magnetism will be classified in this subsection and their magnetic structures and magnetic properties will be described.

The magnetic flux density \vec{B} and the magnetization vector \vec{M} are commonly used in engineering application to describe the magnetization. The relationship between \vec{B} and \vec{M} is

$$\vec{B} = \mu_0(\vec{H} + \vec{M}), \quad (2.10)$$

where μ_0 is the permeability in vacuum and \vec{H} is the magnetic field intensity. The relation between the magnetic field intensity \vec{H} and the magnetization vector \vec{M} can be represented by a linear operator, a nonlinear operator, or a hysteresis operator. However, for linear materials, the relation between the magnetization \vec{M} and the magnetic field intensity \vec{H} can be expressed by

$$\vec{M} = \chi_m \vec{H}, \quad (2.11)$$

where χ_m is the magnetic susceptibility. The observed value of the magnetic susceptibility ranges from 10^{-5} for soft magnetic materials to 10^6 for hard magnetic magnets. The susceptibility is not necessarily constant. It can vary as the function of the applied field. Moreover, the susceptibility does not need to be scalar, it can be also a tensor, to represent anisotropic material, and in some cases it takes negative values as well, e.g. in superconductors. Substituting (2.11) into (2.10), we have

$$\vec{B} = \mu_0(1 + \chi_m)\vec{H} = \mu_0\mu_r\vec{H}. \quad (2.12)$$

The relation between the magnetic induction \vec{B} and the applied field \vec{H} can be expressed by the relative permeability μ_r .

On the basis of the magnetic susceptibility, the magnetic behavior of materials can be classified as diamagnetism, paramagnetism, antiferromagnetism, ferrimagnetism and ferromagnetism [2].

1. Diamagnetism is a weak magnetism in which a magnetization is exhibited opposite to the direction of the applied field. The magnetic susceptibility χ_m is negative and order of magnitude is in general about 10^{-5} . Examples of diamagnetic materials are some rare gases and nonmetallic elements, but some metals, e.g. copper (Cu), silver (Ag), zinc (Zn) and gold (Au) also belong to the diamagnet materials.

2. Paramagnetism is a weak magnetism as well. In paramagnetism, the magnetization \vec{M} is proportional to the magnetic field \vec{H} . Paramagnetic materials contain magnetic atoms or ions whose spins are not compensated. At finite temperatures, the spins are thermally agitated and take random orientations. According to the Curie law, the susceptibility of paramagnetic materials is inversely proportional to the temperature. In the paramagnetic case, the magnetization \vec{M} is increasing with the applied field \vec{H} . The magnetic susceptibility χ_m is positive and its order of magnitude is 10^{-5} to 10^{-3} . Examples of paramagnetic materials are oxygen (O₂), aluminum (Al), manganese (Mn) and the alloys

of the rare earth elements from lanthanum (La) to ytterbium (Yb), and iron (Fe), cobalt (Co) and nickel (Ni).

3. Antiferromagnetism is similar to paramagnetism in the sense of exhibiting a small positive susceptibility. The susceptibility depends on the temperature, as characterized by the occurrence of a kink in the $\chi_m - T$ curve at the Néel temperature T_N (Fig. 2.1 B). According to the interaction between the magnetic moments, an antiparallel spin arrangement is established, in which the plus and minus spins completely cancel each other (Fig. 2.1 A). In such an antiferromagnetic arrangement of spins, the tendency to be magnetized by the external field is opposed by a strong negative interaction acting between plus and minus spins. If there is no external field, the opposite directed moments completely compensate each other. When applying an external field, the antiferromagnetic material proves weak magnetic properties with small positive susceptibilities. The compounds of manganese (MnO, MnS), vanadium (VO₂) and iron (FeS₂) belong to the antiferromagnetic materials.

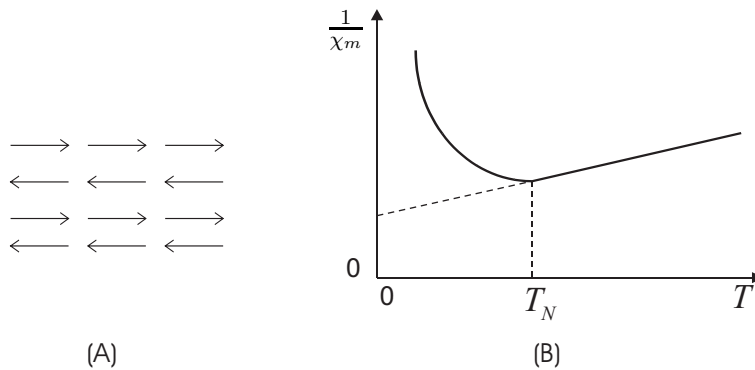


Figure 2.1: Antiferromagnetic material, (A) Configuration of magnetic spins, (B) Temperature dependence of the susceptibility.

4. Ferrimagnetism is the term proposed by Néel² to describe the magnetism of ferrites. In these substances, magnetic ions occupy two kinds of lattice sites, the spins on one site point in the plus direction, whereas those on the other site point in the minus direction. Since the number of magnetic ions and also the magnitude of spins of individual ions are different on the both sites, such an ordered arrangement of spins gives rise to a resultant magnetization, i.e. spontaneous magnetization. As the temperature increases, the arrangement of the spins is disturbed by thermal agitation. Above the Curie point T_C , the substance exhibits paramagnetism, and the susceptibility decreases with increase of temperature (Fig. 2.2). Ferrimagnetism is observed in various kinds of magnetic compounds. In these materials the divalent metal ions can be found as manganese (Mn), cobalt (Co), nickel (Ni), zinc (Zn). The ferrimagnetic garnets are the group of minerals, where the divalent elements are the rare earth materials, such as cadmium (Cd), terbium (Tb), yttrium (Y).

5. In the case of ferromagnetism, the spins are aligned parallel to one another as a result of a strong positive interaction acting between the neighboring spins (Fig. 2.3(A)). As the temperature increases, the arrangement of the spins is disturbed by thermal agitation, thus resulting in a temperature dependence of spontaneous magnetization (Fig. 2.3(B)). Above the Curie point, the susceptibility obeys the Curie-Weiss law, which states that

$1/\chi_m$ rises from zero at the Curie point T_C and increases linearly with temperature as shown in Fig. 2.3(C).

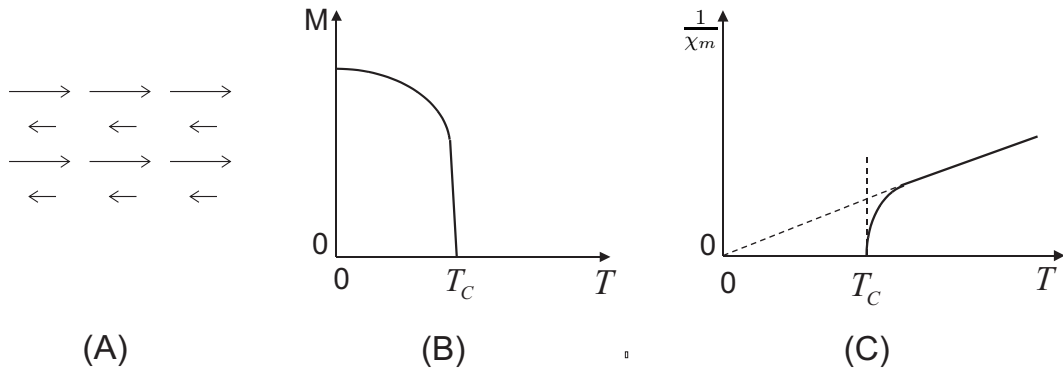


Figure 2.2: Ferrimagnetic material, (A) Configuration of magnetic spins; (B) Spontaneous magnetization; (C) Temperature dependence of the susceptibility.

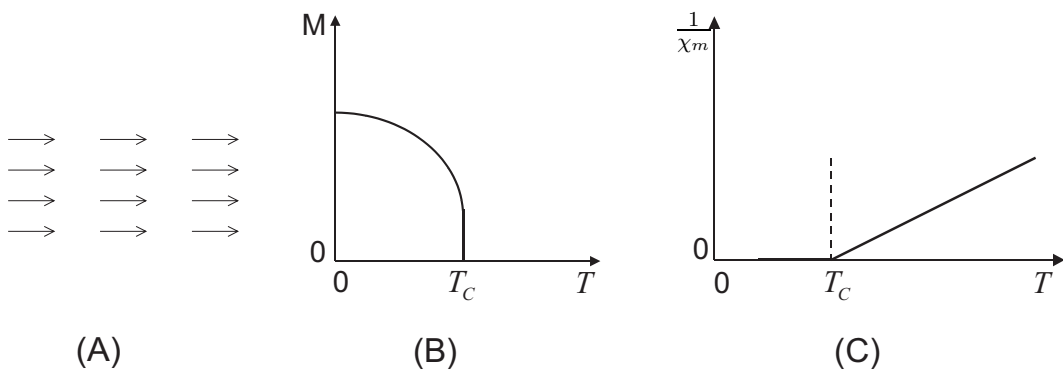


Figure 2.3: Ferromagnetic material, (A) Configuration of magnetic spins; (B) Spontaneous magnetization; (C) Temperature dependence of the susceptibility.

The interior of the ferromagnetic material is divided into many magnetic domains, each of which is spontaneously magnetized. The domain sizes change from a few microns to perhaps millimeters for many ferromagnetic materials. In the domains, a large number of atomic moments, i.e. 10^{12} to 10^{18} , are aligned parallel, so that the magnetization within the domain is almost saturated. Since only the direction of the domain magnetization is varying from domain to domain, the resultant magnetization can be changed from zero to the value of saturation magnetization.

The magnetic properties of a ferromagnetic material are represented by the plot of the magnetization \vec{M} or magnetic flux density \vec{B} at various field intensity \vec{H} , which is shown in Fig. 2.4. In the ferromagnetic materials, the orientation of the domains is randomly distributed. In demagnetized state at absence of the applied field the magnetization is zero